

Basal forebrain dynamics during nonassociative and associative olfactory learning

Sasha Devore,¹ Nathaniel Pender-Morris,¹ Owen Dean,¹ David Smith,² and Christiane Linster¹

¹Department of Neurobiology and Behavior, Cornell University, Ithaca, New York; and ²Department of Psychology, Cornell University, Ithaca, New York

Submitted 9 June 2015; accepted in final form 10 November 2015

Devore S, Pender-Morris N, Dean O, Smith D, Linster C. Basal forebrain dynamics during nonassociative and associative olfactory learning. *J Neurophysiol* 115: 423–433, 2016. First published November 11, 2015; doi:10.1152/jn.00572.2015.—Cholinergic and GABAergic projections from the horizontal diagonal band (HDB) and medial preoptic area (MCPO) of the basal forebrain to the olfactory system are associated with odor discrimination and odor learning, as well as modulation of neural responses in olfactory structures. Whereas pharmacological and lesion studies give insights into the functional role of these modulatory inputs on a slow timescale, the response dynamics of neurons in the HDB/MCPO during olfactory behaviors have not been investigated. In this study we examined how these neurons respond during two olfactory behaviors: spontaneous investigation of odorants and odor-reward association learning. We observe rich heterogeneity in the response dynamics of individual HDB/MCPO neurons, with a substantial fraction of neurons exhibiting task-related modulation. HDB/MCPO neurons show both rapid and transient responses during bouts of odor investigation and slow, long-lasting modulation of overall response rate based on behavioral demands. Specifically, baseline rates were higher during the acquisition phase of an odor-reward association than during spontaneous investigation or the recall phase of an odor reward association. Our results suggest that modulatory projections from the HDB/MCPO are poised to influence olfactory processing on multiple timescales, from hundreds of milliseconds to minutes, and are therefore capable of rapidly setting olfactory network dynamics during odor processing and learning.

olfaction; acetylcholine; GABA; neuromodulation; electrophysiology; basal forebrain

IN ALL SENSORY SYSTEMS, there is evidence that feedforward connections are accompanied by complementary feedback connections, projecting to structures at relatively peripheral positions in sensory pathways (Churchland and Sejnowski 1988, Gilbert and Sigman 2007). Among these projections, basal forebrain inputs are thought to play a major role in sensory processing, attention, and processing of behavioral context, among others (for review see Sarter et al. 2005). Basal forebrain projections expand to many brain areas, including the cortical mantle, limbic areas, and hippocampal and thalamic structures (Gritti et al. 1998; Lamour et al. 1984; Luiten et al. 1987; Zaborsky et al. 1986, 2015). Among basal forebrain nuclei, the horizontal limb of the diagonal band of Broca and medial preoptic area (HDB/MCPO) provide much of the basal forebrain inputs to primary olfactory structures such as olfactory bulb (OB) and piriform cortex (PC). Neurons projecting to

olfactory areas are somewhat, but not exclusively, anatomically segregated from neurons projecting to other sensory and cortical areas (Gritti et al. 1998, 2003; Luiten et al. 1987; Zaborsky et al. 1986, 1999). HDB/MCPO projections to olfactory and other areas are cholinergic, GABAergic, and glutamatergic (Brashear et al. 1986; Zaborsky et al. 1986). Whereas the dynamics of other basal forebrain nuclei during behavior have been investigated (Lin and Nicolelis 2008; Thomson et al. 2014; Tingley et al. 2014), the dynamics of HDB neurons during behavioral tasks have not yet been studied. In this study we recorded from basal forebrain neurons during two olfactory behaviors, one spontaneous and one reward driven.

Numerous studies have demonstrated the importance of the projections from HDB/MCPO to olfactory structures in a variety of olfactory learning and memory tasks. Typically, these studies involve manipulation of the HDB/MCPO projections either directly within the HDB/MCPO through immunological lesions (De Rosa et al. 2001; Linster and Cleland 2002; Linster et al. 2001), molecular pharmacology (Nunez-Parra et al. 2013), or pharmacological block of the target receptors via systemic injections or local infusions into the recipient olfactory networks (Chapuis and Wilson 2013; Chaudhury et al. 2009; Devore et al. 2012, 2014; Mandairon et al. 2006; Pavese et al. 2013), or through genetic manipulations of targeted receptors (Abraham et al. 2010; Nunez-Parra et al. 2013; Nusser et al. 2001). All of these techniques disrupt the HDB/MCPO signaling to olfactory structures on a long timescale, from tens of minutes to permanently. Thus the time course of the HDB/MCPO projections and how they are involved in specific task-related behaviors cannot be discerned from previous studies. Moreover, it is not known how activity in basal forebrain neurons correlates with olfactory behaviors.

In the present study, we address this question by recording directly from neurons in the HDB/MCPO in rats performing olfactory learning and memory tasks, including a nonassociative novel odor investigation task and a reward-motivated two-alternative forced-choice (2AFC) odor discrimination task. Similarly to what has been reported from other basal forebrain nuclei (Hangya et al. 2015; Lin and Nicolelis 2008; Thomson et al. 2014; Tingley et al. 2014), we observe rich heterogeneity in the response dynamics of individual HDB/MCPO neurons, with a substantial fraction of neurons exhibiting task-related modulation.

MATERIALS AND METHODS

General Methods

Animal subjects. Adult male Long-Evans rats, obtained from Charles River Laboratories (Wilmington, MA) and weighing 300–

Address for reprint requests and other correspondence: C. Linster, Computational Physiology Lab, Dept. of Neurobiology and Behavior, Cornell Univ., Ithaca, NY 14853 (e-mail: cl243@cornell.edu).

350 g, were used in the study. Rats were individually housed in standard laboratory cages in a temperature- and humidity-controlled environment and kept on a 12-h reverse light cycle, with lights off between 0900 and 2100. All behavioral testing took place between 1000 and 1600. Procedures and protocols were approved by the Cornell University Institutional Animal Care and Use Committee and were in accordance with National Institutes of Health guidelines.

Odorants. Odors used in this study were drawn from a large battery consisting primarily of carboxylic acids, aliphatic aldehydes, esters, and ketones obtained from Sigma-Aldrich (St. Louis, MO). Pure odors were diluted in mineral oil so as to theoretically emit a vapor-phase partial pressure of 1 Pa (Cleland et al. 2002). Table 1 lists all odors used in these experiments together with their corresponding liquid-phase dilutions.

Behavioral apparatus. All training and testing occurred in an opaque Plexiglas chamber (24 × 12 × 18 in.) with gently sloping (~15°) walls. Two holes (2-in. diameter) were cut into the far wall of the chamber at a height of 2 in. from the ground; a removable divider restricted access to the holes during behavioral testing. An infrared photosensor (Omron Electronics, Danvers, MA) was installed at the base of the divider to automatically register opening and closing of the divider. A video camera (Microsoft LifeCam VX-2000) mounted above the box was used to record and monitor behavioral sessions. Video was acquired at a rate of 30 frames/s using the Spike2 video recording utility (Cambridge Electronic Devices, Cambridge, UK).

Surgery. Under aseptic conditions, rats were anesthetized with isoflurane (5% saturated vapor) and mounted in a stereotaxic apparatus. Anesthesia was maintained throughout the surgical procedures with isoflurane at 1–3% saturated vapor. The skull was exposed by a midline incision, and the overlying tissues were removed. A small craniotomy (~2-mm diameter) was made in the skull, and a custom-built microdrive was stereotaxically implanted ~300 μm dorsal to the HDB/MCPO (from Bregma: -0.3 mm anteroposterior, 1.8 mm mediolateral, 8.0 mm dorsoventral). The microdrive housed two bundles of four wires, each consisting of four tightly wound 17-μm platinum-iridium (Pt-Ir, 90/10%) microwires or 25-μm stainless steel wires (California Fine Wire). Initially, rats were implanted with Pt-Ir wire, but stainless steel wires were found to result in more reliable HDB/MCPO neuron isolation, so the remaining rats were implanted with 25-μm stainless steel wire. Before surgical implantation, the Pt-Ir microwires were cut and plated with platinum to reduce impedances to 200–400 kΩ at 1 kHz; the stainless steel microwires were cut but not plated and had nominal impedances of 500–700 kΩ at 1 kHz. The microdrive was secured to the skull using stainless steel bone screws and dental acrylic. A Teflon-coated silver wire (A-M Systems; Sequim, WA), connected to one of the bone screws, served as ground. The animals were administered the analgesic ketoprofen (5 mg/kg) subcutaneously both at the start of the surgical procedure and again 8 h postsurgery. Rats were allowed to recover for 1 wk following surgery before commencing behavioral training.

Electrophysiology. Electrophysiological signals were obtained using a system similar to that of Chaudhury et al. (2009), which was adapted for recordings in awake, behaving rodents. Briefly, neural activity was recorded through an HS-27 head stage connected to a Neuralynx ERP-27 panel with a Lynx-8 amplifier (Neuralynx, Tucson, AZ). The raw signals were amplified and filtered to isolate spiking activity (5,000×, 600–6,000 Hz), digitized at a sampling rate of 20 kHz using a CED Power1401 interface and Spike2 software (Cambridge Electronic Design), and stored onto a computer disk for offline analysis. All data acquisition for the behavioral experiments, including both electrophysiological and video recording, was done within Spike2 to synchronize time stamps. At the end of each session, electrodes were advanced by at least 40 μm by rotating the drive legs; a complete revolution lowered the electrodes by 320 μm. We advanced electrodes no more than 1,280 μm (i.e., 4 revolutions) from their original position to avoid recording ventral to the HDB/MCPO and to facilitate identification of recordings within the target region.

Table 1. *Odorants used in Experiments 1 and 2*

Odorant	%Vol/Vol	Experiment	
		1	2
Acetic acid	0.0078	*	
Propanoic acid	0.033	*	*
Pentanoic acid	0.45	*	*
Hexanoic acid	1.488	*	*
Heptanoic acid	4.627	*	*
Octanoic acid	13.742	*	
Methyl acetate	0.00426	*	
Ethyl acetate	0.00169	*	
Butyl acetate	0.0219	*	*
<i>N</i> -propyl acetate	0.00627	*	
<i>N</i> -amyl acetate	0.0723	*	*
Hexyl acetate	0.227	*	*
Butyl propionate	0.0604	*	*
Butyl pentanoate	0.572	*	*
Butyl hexanoate	1.627	*	*
Methyl butyrate	0.0071	*	*
Ethyl butyrate	0.0181	*	*
Propyl butyrate	0.0522	*	*
Butyl butyrate	0.165	*	*
Pentyl butyrate	0.572	*	
Hexyl butyrate	1.627	*	*
Methyl 2-furoate	0.247	*	
Methanol	0.000309	*	
Furfuryl propionate	0.651	*	
Ethyl pentanoate	0.0598	*	*
Methyl valerate		*	
Butanol	0.0208	*	
Propanol	0.00553	*	
Pentanol	0.0744	*	*
Hexanol	0.255	*	*
Heptanol	0.838	*	*
1-Octanol	2.673	*	*
3-Heptanone	0.0646	*	*
2-Heptanone	0.0574	*	
2-Pentanone	0.0054	*	*
2-Furyl methyl ketone	0.259	*	
2-Hexanone	0.0180	*	
5-Methylfurfural	0.299	*	
Citronellal	1.658	*	
Butanal	0.00185	*	
Propanal	0.000485	*	
Pentanal	0.00657	*	*
Hexanal	0.0221	*	*
Heptanal	0.0707	*	*
Octanal	0.147	*	*
1,8-Cineole	0.195	*	
+Terpenin	6.632	*	
Anisole	0.0515	*	
Eugenol	0.0746	*	
+Carvone	4.716	*	
+Limonene	0.204	*	

All odorants were diluted in mineral oil to theoretically emit a vapor-phase partial-pressure of 1 Pa; the resulting percent volume/volume (%vol/vol) concentrations are listed. Odorants were used in either *Experiment 1* only or in both *Experiments 1* and 2, as indicated by asterisks in the rightmost columns.

Single units were extracted from raw waveforms using the Spike2 spike-sorting package, which uses principal components analysis as well as wave-shape features. We assessed the quality of spike sorting by examining interspike interval (ISI) histograms as well as waveform stability; units were considered to be well isolated if fewer than 2% of the spikes fell within a 2-ms refractory period. Typically, we extracted one to two single units across all channels during a single recording session. Spike times as well as time stamps of behavioral events were exported from Spike2 and further analyzed using custom-written scripts in MATLAB (The MathWorks, Natick, MA).

Histology. When they completed behavioral testing, rats were deeply anesthetized with urethane and killed via cardiac perfusion of 0.9% saline followed by 10% formalin solution. In animals implanted with stainless steel electrodes, we first passed anodal current (10 μ A, 20 s) through one of the implanted microwires and then perfused a solution of 1% potassium ferrocyanide to produce a Prussian blue reaction. Brains were extracted, saturated in a solution of 30% sucrose in PBS, and then sectioned into 40- μ m slices and stained with cresyl violet or neutral red to assess electrode placement. Only animals with electrode placement within the vicinity of the HDB/MCPO were included in data analysis (Fig. 1A). Figure 1B shows an example section from one of the experimental animals illustrating an electrolytic lesion terminating in the HDB/MCPO.

Experiment 1: Spontaneous Odor Investigation

Animal subjects. Ten rats were used in *Experiment 1*. Rats were allowed unlimited access to water but were kept on a food restriction schedule to prevent obesity.

Behavior. Animals were gradually acclimated to the behavioral apparatus over the course of 1 wk before undergoing microdrive implantation surgery. At the end of the postoperative recovery period, rats were reintroduced to the behavioral chamber for 1–3 days before behavioral test sessions commenced. Rats were allowed to acclimate to the behavioral chamber for 15 min at the start of every test session, followed by 8–16 experimental trials using a randomly selected set of odorants not previously encountered by the subject in the task (Fig. 2A). Trials were separated by 3-min intertrial intervals (ITI). At the start of each trial, 60 μ l of a novel odorant were placed on a piece of filter paper inside a mesh tea ball. The odorized tea ball was pushed into one of the odor ports at the far wall of the chamber; the other odor port contained an identical, nonodorized tea ball. The chamber divider was lifted, allowing rats to access the tea ball during a 60-s odor

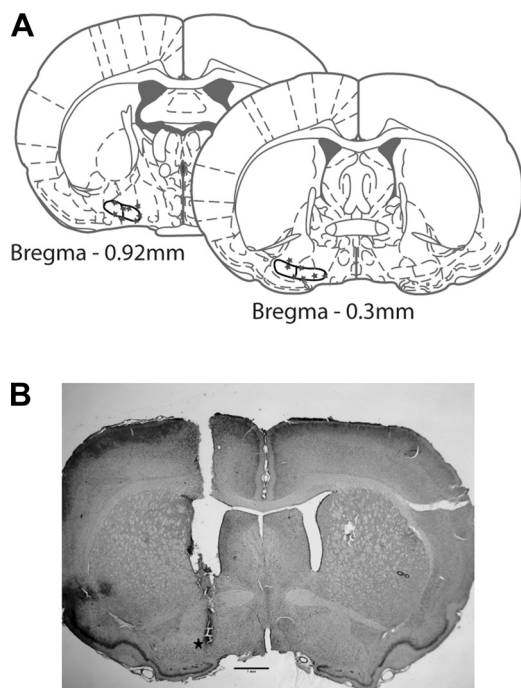


Fig. 1. Reconstruction and verification of anatomical recording sites within the horizontal limb of the diagonal band of Broca (HDB) and medial preoptic area (MCPO). **A:** histological reconstruction of recording sites within the nucleus of the HDB/MCPO. Target structure is indicated by thick black lines. Anatomical plates adapted from Paxinos and Watson (2007) represent the approximate extent of reconstructed sites along the rostrocaudal axis. **B:** photomicrograph showing an electrode track terminating in an electrolytic lesion within the HDB/MCPO (indicated by star).

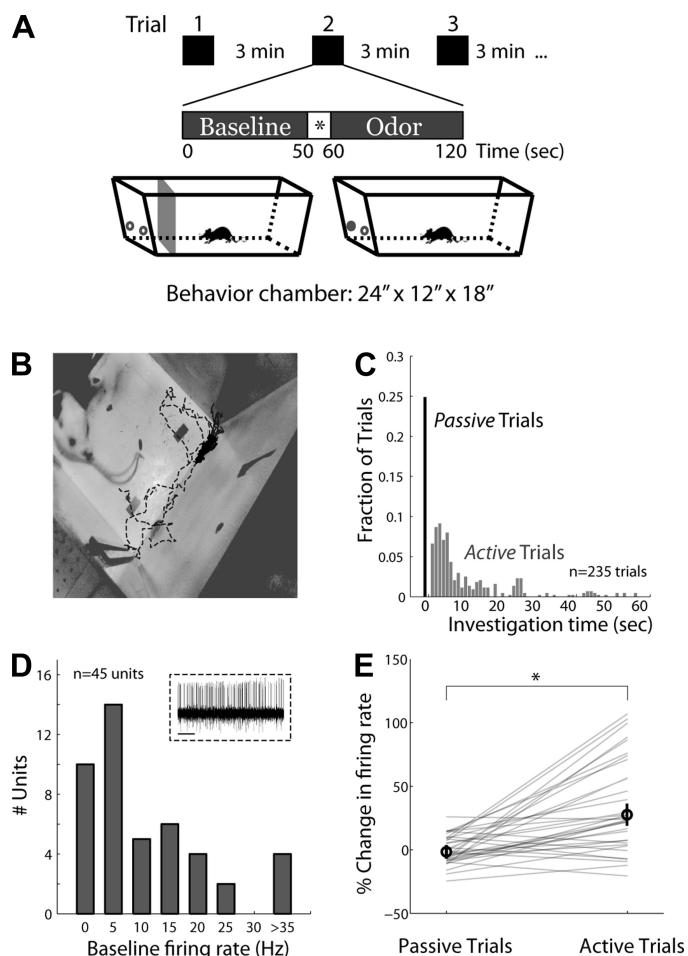


Fig. 2. Neural activity in the HDB/MCPO during a nonassociative odor investigation task. **A:** task overview and schematics of the behavioral setup. Trials consisted of a 1-min baseline epoch followed by a 1-min novel odor presentation. Trials were separated by 3-min intervals. During the intertrial interval and baseline epoch, access to the odor ports was blocked by an opaque divider. Immediately before the start of the odor epoch, a novel odor stimulus was loaded into one of the odor ports (circles) and the divider was lifted to allow rats access to the odor port for 60 s. **B:** example nose-tracking run during the odor epoch for a single trial. Dashed line shows the position of the rat's nose; dots indicate times at which the rat was engaged in directed odor investigation. **C:** histogram of total investigation time for each trial, across all rats and behavioral sessions. Trials with no investigation were defined as “passive” or exposure trials, whereas trials with any investigation greater than zero were defined as “active” or odor investigation trials. **D:** histogram of average firing rates during the baseline epoch for all recorded HDB/MCPO neurons. *Inset:* example activity trace obtained from a single site in the HDB/MCPO. **E:** average change in firing rate relative to baseline for each unit, plotted separately for passive and active trials. Across the population, there was a significant increase in activity during the odor epoch on active compared with passive trials (* $P < 0.001$). Error bars denote SE ($n = 45$).

exposure period. The experimenter logged the start of the trial electronically by pushing a button on the keyboard. This triggered a timer, which automatically logged (and silently indicated) the end of the trial. At the end of the odor exposure period, the rat was moved to the far side of the chamber, the divider was put back in place, and the tea balls were removed. The location of the odorized and neutral tea balls were fixed throughout the duration of a test session but were randomized across test sessions.

Analysis. BEHAVIORAL DATA ANALYSIS. All behavioral analysis was performed offline using the videos recorded during the behavioral test sessions. Using custom-written MATLAB routines, we manually marked the position of the subject's nose in each video frame and

measured the amount of time subjects actively investigated the odorant. Active investigation was defined as directed sniffing within 1 cm of the odor tea ball. Individual trials were classified as active or passive according to the active investigation time over the course of the trial. Namely, passive trials were defined as those trials in which the investigation time was zero, whereas active trials were those in which the investigation time was anything nonzero (Fig. 2, *B* and *C*). Furthermore, within a given trial, we labeled each time epoch as a period of directed investigation or not. Periods not defined as directed investigation could include other behaviors such as, for example, grooming, quiescence, or wandering.

ELECTROPHYSIOLOGICAL DATA ANALYSIS. Neural signals were recorded in 3-min intervals starting 60 s before and ending 60 s after the odor exposure period. Each trial was split into baseline and odor epochs based on the time stamps for the start and stop of the odor exposure period (Fig. 2A). All analyses excluded activity in a 10-s window preceding the start of the odor investigation to avoid contamination due to, for example, noise and visual signals generated by the placement of the odor sources. We computed the average firing rate during each epoch by summing the number of action potentials and dividing by the epoch duration. We also computed the average firing rate during active investigation by using the frame-by-frame video analysis to define periods of odor investigation within the odor epoch. For each individual cell, we used paired *t*-tests to determine if there were significant differences in firing rate between epochs (odor vs. baseline) or during active investigation. The significance level for all statistical testing was set to $\alpha = 0.05$.

Experiment 2: Forced-Choice Odor Discrimination

Animal subjects. Six rats were used in *Experiment 2*. Rats were allowed unlimited access to water but were kept on a food restriction schedule to maintain their body weight at 85–90% of their free-feeding body weight.

Training. Rats were shaped to acquire 45-mg odorless, dustless sucrose pellets (Bio-Serv, Frenchtown, NJ) from a 1.5-cm depression in the center of a sponge fitted inside a ceramic ramekin cup (8-cm diameter, 4.5-cm height). The sponge-ramekin assembly is referred to as an “odor pot.” The rat was kept on one side of the chamber and, after the divider was lifted, was trained to approach the odor pot located at the opposite end of the chamber. Training was considered complete when rats would reliably, with a <5 s pause, approach the odor pot and retrieve the sucrose pellet. All rats used in this study completed training within 2–3 days. After completion of pellet training, rats were allowed ad libitum access to food and water for 1 wk before undergoing microdrive implantation surgery (as described above). Following a 1-wk postoperative recovery period, rats again underwent food deprivation and pellet training to prepare them for behavioral testing.

Behavior. Rats performed a 2AFC olfactory discrimination task. For each discrimination problem, a novel pair of odors (A and B) was selected from the list of possible odorants (see Table 1). Rats learned to discriminate either the two pure odorants, A and B, or binary mixtures of the two odorants in the ratio 2A:1B vs. 1A:2B. In each discrimination problem, one of the odors was randomly assigned as the rewarded odor. During testing, odorants were delivered by pipetting 60 μ l of odorant onto the sponges in the odor pots. The rewarded odor pot contained a sucrose pellet in the sponge depression. A single experimental session consisted of one or two novel discrimination problems. Animals completed 40 trials for each discrimination problem. For each trial, the location of the rewarded odor pot (i.e., left vs. right) was randomly assigned before testing to control for side bias by the animal. A trial commenced when the divider was lifted, allowing the rat to move forward and approach the odor pots. A rat was considered to have made a decision if it lowered its nose into one of the two sponge depressions. Rats were not allowed to self-correct. Immediately following the initial decision, the ceramic pots were

removed, the rat was moved to the other side of the chamber, and the divider was inserted. The ITI was 25 s following correct trials and 45 s following incorrect trials. All sessions were video recorded, as described above, to enable offline definition of behavioral epochs.

After completion of all experimental sessions, animals performed a control task to determine whether they could use visual or odor cues from the sucrose pellet to guide behavior. In this task, the odor [(+)-limonene] was identical in rewarded and unrewarded odor pots so that the only cues from the task came directly from the sucrose pellet. As in experimental testing, the placement of the rewarded odor pot, left or right, was randomized for these trials.

Analysis. BEHAVIORAL DATA ANALYSIS. Performance was assessed by computing the fraction of correct trials over the duration of the entire discrimination task as well as in blocks of 10 trials. Asymptotic performance was defined as the success rate in the final five trials. To quantify learning rate for a particular discrimination problem, we defined criterion performance as $\geq 80\%$ correct for two consecutive blocks of ten trials, computed using a sliding window with 50% overlap.

ELECTROPHYSIOLOGICAL DATA ANALYSIS. Neural signals were recorded continuously throughout the duration of each discrimination task. Each trial was split into four distinct epochs based on information obtained from the photosensor and the position of the rat, which was manually determined from the recorded video files using custom-written MATLAB routines. We defined two active behavioral epochs: trial start commenced when the divider was lifted and odor investigation began when the subject's nose reached the edge of the odor pots. The odor investigation epoch ended when the rat made a decision and lowered its nose into one of the sponge depressions. In addition, we defined a baseline epoch that overlapped with the ITI. The end of each epoch coincided with the start of the subsequent epoch, with the exception of the baseline epoch, which ended 5 s before the divider was lifted to exclude activity related to odor pot placement or experimenter movement.

For each trial, we computed an epoch-related firing rate by dividing the total number of spikes by the epoch duration. We used paired *t*-tests to determine if there were significant differences in activity during the active behavioral epochs relative to baseline. We then performed separate analyses to detect whether there were differences in activity during learning. We first determined if there were significant changes in baseline activity during learning by comparing firing rates on pre- and postcriterion trials using an unpaired *t*-test. To examine differences between active behavioral epochs before and after learning, we first expressed relative firing rates in each epoch by subtracting the baseline firing rate and then used unpaired *t*-tests to compare epoch-related modulations in activity between pre- and postcriterion trials. The significance level for all statistical testing was set to $\alpha = 0.05$.

RESULTS

Projections from the HDB/MCPO, in the basal forebrain, to the OB and olfactory cortex are critical for various forms of olfactory learning and memory (for review, see Devore and Linster 2012; Fletcher and Chen 2010; Wilson et al. 2004). In this work, we studied the activity of HDB/MCPO neurons during olfactory behaviors by recording from awake, freely moving and behaving rats.

Neural Activity in the HDB/MCPO is Modulated by Active Odor Investigation

In studies of perceptual odor discrimination, freely moving animals are habituated to an odor across repeated presentations and discrimination is assessed by the extent to which animals investigate novel test odorants (Cleland et al. 2002). Disrupting

either the cholinergic or GABAergic HDB/MCPO projections to the olfactory system impairs perceptual discrimination of chemically similar odors (Abraham et al. 2010; Mandairon et al. 2006; Nunez-Parra et al. 2013; Nusser et al. 2001). As a consequence, in our first set of experiments, we determined the dynamics of HDB/MCPO activity during olfactory perceptual learning by recording from cells ($n = 45$) located in the region of the HDB/MCPO in awake, freely moving rats ($n = 9$) engaged in a nonassociative, novel odor investigation task. The behavioral paradigm consisted of a series of 60-s odor exposure trials separated by 4-min ITIs. During the ITI, a barrier panel kept rats on the far side of the test chamber (Fig. 2A). At the start of each novel odor trial, the barrier panel was lifted so that the rats could access the odor ports for 60 s (odor epoch). Throughout the odor epoch, rats were allowed to freely roam the behavior chamber; odor investigation was based on rats' propensity to investigate novel sensory stimuli. This paradigm has been used extensively by our laboratory and others to investigate odor memory formation and spontaneous odor discrimination (reviewed in Wilson and Linster 2008).

We defined a baseline activity epoch as the 60 s preceding the odor exposure period (Fig. 2A). Firing rates during the baseline period varied substantially across the population of recorded neurons (Fig. 2D), with a mean firing rate of 11.05 ± 11.02 Hz; these values are comparable to those previously observed in anesthetized animals (Linster and Hasselmo 2000).

Using frame-by-frame video analysis, we then extracted active odor investigation during the odorant-exposure epoch and found that in the majority of trials, animals approached the odor source to investigate during the odor epoch (see example track in Fig. 2B), although in $\sim 25\%$ of the trials (62/235), animals remained on the ITI side of the test chamber. Figure 2C displays the histogram of investigation times across all trials and animals. We classified individual trials as active trials if the animal had at least one frame of active investigation; all other trials, with zero investigation time, were labeled passive odor trials. We examined firing rates, relative to baseline, separately for passive and active trials for each unit in our sample. The firing rate during the odor epoch was significantly higher in active trials compared with passive trials in 14/45 neurons (average increase 1.75 ± 1.5 spikes/s); in the remainder of neurons (31/45) there was no significant change. At the population level, firing rates increased relative to baseline on active trials ($P < 0.001$, paired t -test; Fig. 2E), whereas during passive trials there was no significant change from baseline ($P = 0.71$, paired t -test; Fig. 2E). These results show that firing rates of HDB/MCPO neurons are modulated during active odor investigation.

We next analyzed neurons' responses during active trials in more detail to determine if firing rates were modulated specifically strongly during the short bouts of active sniffing of the odor source. To do this, we compared firing rates during bouts of active odor investigation on active trials (determined using video analysis) to firing rates throughout the remainder of the active trial. Figure 3A shows an example raster plot for a neuron that exhibited substantial increases in activity during bouts of directed odor investigation (denoted by thick blue lines above each trial row). In contrast, Fig. 3B shows data from a neuron in which the firing rate decreased during bouts of active odor investigation. Across the population, the activity of 12 neurons (27%) was significantly different during bouts of

directed investigation compared with all other times within the same trial. In 75% of these neurons (9/12), activity increased during investigation; on average, activity in these neurons nearly doubled during periods of active investigation, with an average increase of 9.59 ± 4.76 spikes/s. In the remaining 25% (3/12), activity decreased (average decrease = 3.18 ± 0.41 spikes/s). Figure 3C shows the differences in activity during periods of no sniffing and sniffing for all units in the population. This analysis of the relationship between HDB/MCPO activity and active odor investigation strongly suggests a role for basal forebrain activity in odor perception.

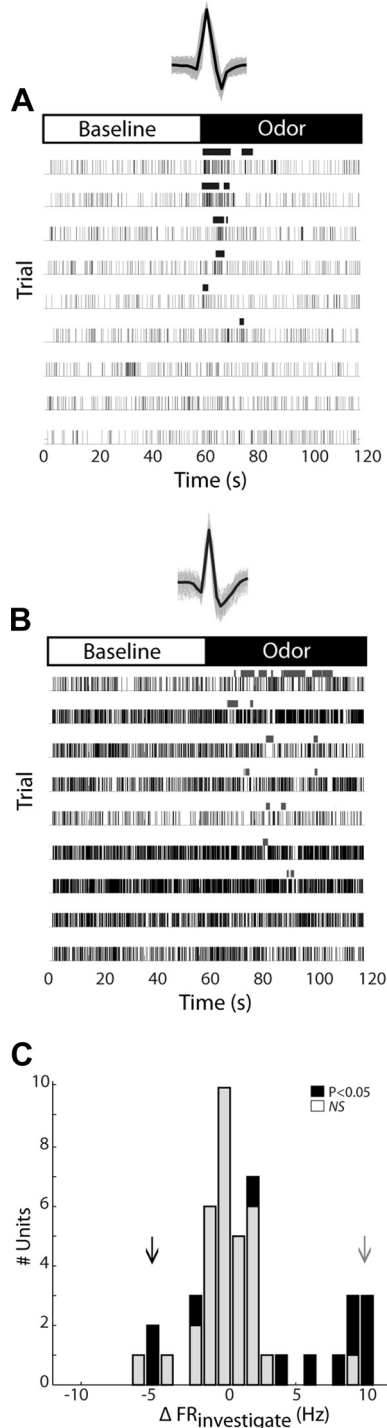
Neural Activity in the HDB/MCPO During Reward-Motivated Learning Reflects Odor Learning

In addition to playing a prominent role in sculpting olfactory discrimination during nonassociative odor discrimination tasks (Mandairon et al. 2006; Nunez-Parra et al. 2013), basal forebrain inputs to the olfactory system have been implicated in a diverse array of reward-motivated olfactory learning and behaviors (reviewed in Devore and Linster 2012; Wilson et al. 2004). Therefore, in *Experiment 2*, we characterized response dynamics of HDB/MCPO neurons ($n = 42$) in a separate cohort of rats ($n = 6$) trained to perform a 2AFC olfactory discrimination task. On each trial, rats were presented with two odorants contained in ceramic dishes and had to retrieve a sucrose pellet from the dish containing the rewarded odorant (Fig. 4A). Rats experienced a new set of odors on each testing day ($n = 22$ sessions). As a result, performance was near chance at the beginning of each behavioral session and improved to an accuracy of $>90\%$ as rats acquired the new discrimination problem (Fig. 4B). The learning rate varied across rats and odor sets, with an average of 15.64 ± 6.48 trials to criterion performance (Fig. 4C; see MATERIALS AND METHODS).

HDB/MCPO Neurons Are More Active During Reward-Motivated Behavior

To analyze neural recordings, we split each trial into baseline, trial start, and odor investigation epochs based on specific task-related events (Fig. 4A). Across the population ($n = 42$ cells), the average firing rate during the baseline epoch in all trials was 22.2 ± 20.1 Hz, which was significantly higher than the average firing rate observed in non-food-deprived rats performing the nonassociative spontaneous odor investigation task (Fig. 4D; unpaired t -test, $P = 0.002$). These results indicate that the baseline state of the basal forebrain network is markedly different between the two experimental paradigms. Moreover, in contrast to the nonassociative odor investigation task, in which only a fraction of HDB/MCPO neurons exhibited significant changes in activity between trial epochs, nearly all neurons recorded in the 2AFC odor discrimination task exhibited some type of modulation across trial epochs (38/42 units). The normalized perievent time histograms (PETH) for all 42 units recorded in the HDB/MCPO during the odor discrimination task are displayed in Fig. 4E. Each row corresponds to a single neuron, and each column shows the normalized PETH computed by aligning trials to a specific event, as indicated. From these data it clearly can be seen that neural activity is not uniform throughout the trial, but rather is modulated during specific behavioral epochs. Overall, HDB/MCPO neurons are more engaged during reward-driven be-

haviors, as evidenced by higher baseline firing rates and the larger fraction of neurons whose activity was modulated during the behavioral trials. In the population of cells recorded, modulation of activity during different behavioral epochs was not correlated; for example, of 42 cells reported, 19 showed the same modulation (increase, decrease, or no change) of activity during approach and odor investigation, whereas 23 cells showed different modulation during these epochs. We therefore present the recorded changes in neural activity for each task phase independently.



Most HDB/MCPO Neurons Exhibit Task-Related Enhancement or Suppression at the Start of Each Trial

Figure 5 shows data from three HDB/MCPO neurons illustrating the diversity in neural dynamics exhibited around the start of the trial. The start of each trial was defined as the instant that the chamber divider was lifted, and was directly recorded by a photobeam. In many neurons we observed transient responses locked to the trial start that included either an increase (Fig. 5A) or decrease (Fig. 5B) relative to baseline. In other neurons, the trial onset-locked changes in neural activity were tonic and lasted throughout the duration of the trial (Fig. 5C); the tonic changes were observed in both positive and negative directions relative to baseline. We quantitatively analyzed trial start-related activity by comparing activity in the trial start epoch to baseline on a trial-by-trial basis (Fig. 5D) and found significant effects in 31 of 42 neurons ($P < 0.05$, paired t -test); of these 31 neurons, $\sim 68\%$ (21/31) exhibited a decrease in activity at the start of the trial (average $-31.67 \pm 13.1\%$), and the remaining 10 exhibited an increase (average $46.83 \pm 31.6\%$). The direction of change was correlated with the baseline firing rate such that neurons with overall lower baseline rates tended to increase their firing rates during approach, whereas neurons with higher firing rates tended to exhibit decreases (Fig. 5D).

HDB/MCPO Firing Is Strongly Modulated During Odor Perception and Decision Making

Figure 6 shows data from three HDB/MCPO neurons illustrating the diversity in neural dynamics exhibited during the odor investigation period, which started when the rat's nose entered a 1-cm radius surrounding the odor dishes and ended when the rat made its response selection. Similar to the heterogeneity observed when activity was locked to the trial onset, we observed diversity in the responses of HDB/MCPO neurons during the odor investigation period (Fig. 4E). In some neurons, the response sharply increased (Fig. 6A) and remained elevated across the duration of the investigation period, whereas in others the response exhibited a tonic decrease (Fig. 6B). Some neurons exhibited complex response patterns in-

Fig. 3. Neural activity in the HDB/MCPO related to active odor investigation. *A*: raster plot for an HDB/MCPO neuron that exhibited a significant increase in firing rate during active odor investigation (28.2 Hz) compared with the remainder of the trial (19.1 Hz). Each row denotes an individual trial with a novel odor; thick lines above each row indicate the periods of directed odor investigation, determined from video tracking. Trials are aligned on the start of the odor epoch, denoted by the blocks above the raster. The trials are sorted according to overall investigation time. Individual spike waveforms ($n = 100$) shown together with the average spike waveform (thick black line) at the top of the panel. *B*: raster plot for an HDB/MCPO neuron that exhibited a significant decrease in firing rate during directed odor investigation (9.38 Hz) compared with the remainder of the trial (14.86 Hz). Each row denotes an individual trial with a novel odor; thick lines above each row indicate the periods of directed odor investigation, determined from video tracking. Trials are aligned on the start of the odor epoch as indicated by the blocks above the raster. The trials are sorted according to overall investigation time. Individual spike waveforms ($n = 100$) are shown together with the average spike waveform (thick black line) at the top of the panel. *C*: histogram of the change in firing rate during odor investigation ($\Delta FR_{\text{investigate}}$) for each neuron in our HDB/MCPO population. Shaded bars indicate neurons with $\Delta FR_{\text{investigate}}$ that are significantly different from zero. Arrows correspond to firing rate differences exhibited by the neurons shown in *A* and *B*, respectively. NS, no significance.

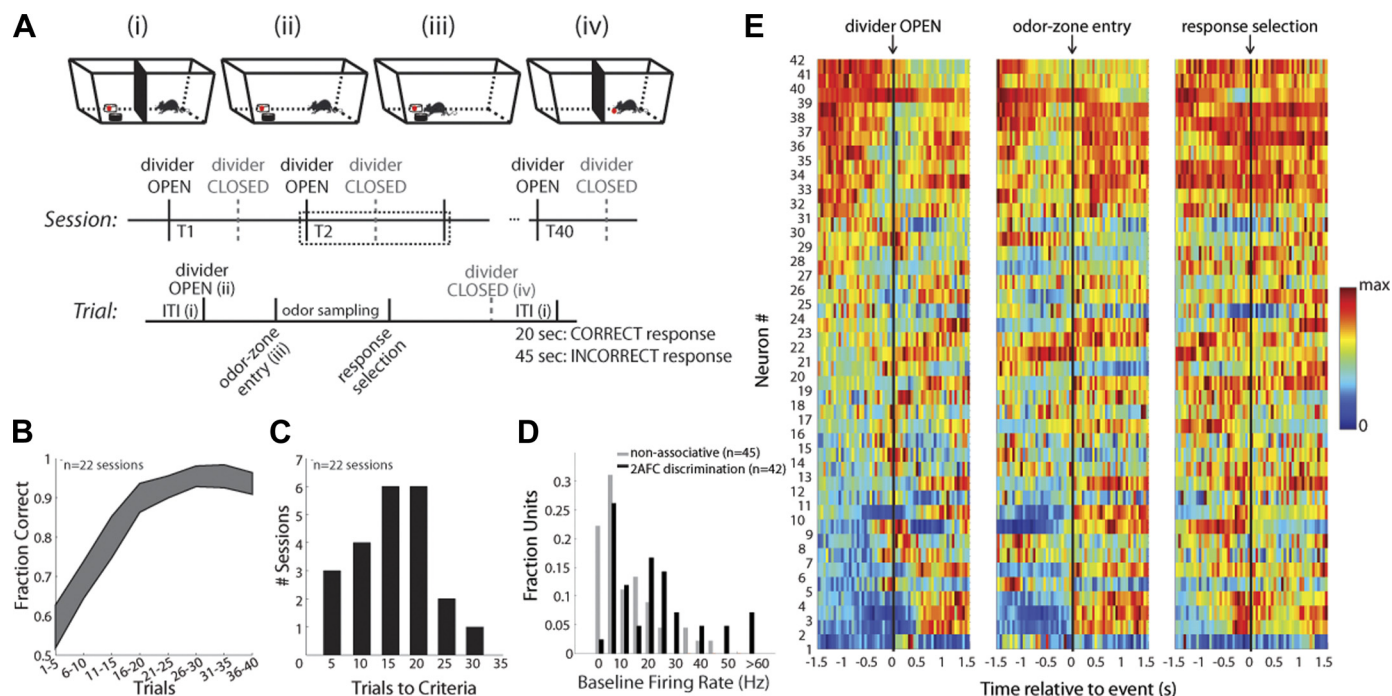


Fig. 4. Neural activity in the HDB/MCPO during two-alternative forced-choice (2AFC) odor discrimination. *A*: task overview and schematic of the experimental setup. Each trial (*bottom row*) begins with the rat on the holding side of the chamber, and then the divider is lifted and the rat approaches the odors, investigates, and selects a response by poking its nose into the dish to search for the reward. Immediately following response selection, rats are moved back to the far side of the chamber and the divider is replaced. During each 2AFC session, rats completed 40 trials using a novel odor set. *B*: average performance of rats on novel 2AFC discrimination problems. Shaded region indicates average \pm SE, computed across all sessions in all rats. *C*: histogram showing the number of trials to reach criterion performance (defined in MATERIALS AND METHODS) for each novel 2AFC experimental session. *D*: histograms of baseline firing rates in HDB/MCPO neurons of rats performing the nonassociative odor investigation task (solid line, $n = 45$ neurons) and 2AFC odor discrimination task (dashed line, $n = 42$ neurons). The average baseline firing rate is significantly higher in the 2AFC rewarded odor discrimination task ($P = 0.007$, unpaired t -test). *E*: normalized perievent time histograms (PETH), computed relative to the 3 major events defining a trial: divider open (*left*), odor zone entry (*middle*), and response selection (*right*). Each row shows the PETH for a single neuron, computed across all 40 trials in the experimental session and normalized to the maximum firing rate in the PETH. Rows are ordered according to the normalized firing rate during the baseline period (i.e., intertrial interval); adjacent rows display data from the same neuron.

cluding phasic as well as tonic changes in activity (Fig. 6C). Across the population, $\sim 75\%$ (32/42 neurons) showed significant changes in activity relative to baseline during the odor epoch (Fig. 6D). There were almost equal incidences of increases and decreases in activity, with 15 of the 32 neurons showing increased activity and 17 of the 32 neurons showing decreased activity. Table 2 summarizes the changes observed across the population of HDB/MCPO neurons during the trial start and odor epochs. Because of the low error rate (6.1 ± 3.2 average number of errors across all trials), we did not analyze whether neural activities during approach or odor investigation epochs differed between correct and incorrect trials.

Modulatory Inputs from HDB/MCPO Decrease When Odor Discrimination Has Been Acquired

Previous studies have suggested a critical role for basal forebrain inputs to the olfactory system in mediating acquisition, but not recall, of olfactory discrimination problems (Chapuis and Wilson 2013; Devore et al. 2014). We therefore tested how HDB/MCPO neural activity is modulated over the course of odor discrimination learning. For each learning session, we split the trials into pre- and postlearning groups based on the trial at which rats reached criterion performance (see MATERIALS AND METHODS). Figure 7, *B* and *C*, illustrates the PETH for three neurons that exhibit differences in activity with learning. The PETH are plotted relative to the start of odor

investigation. We first analyzed changes in baseline activity with learning to determine whether the overall output changes with learning. Figure 7*A* shows a histogram of the change in baseline firing rate with learning, i.e., postcriterion baseline minus precriterion baseline. Postcriterion baseline firing rates were significantly different in $\sim 30\%$ (12/42) of the neurons in our population ($P < 0.05$, t -test). Of these, the majority of neurons (9/12) exhibited a decrease in baseline activity postlearning (average $27.5 \pm 16.2\%$); the remaining 3 neurons showed modest increases (average $22.6 \pm 12.4\%$). These results, which demonstrate that baseline activity in the HDB/MCPO decreases once an animal reaches criterion performance on an odor discrimination task, suggest that the strength of neuromodulatory inputs from the basal forebrain to the early olfactory system may, in part, be regulated by learning.

To determine if there were learning-related differences in HDB/MCPO response dynamics beyond overall shifts in baseline activity, we next analyzed whether the approach- and odor-related activity levels changed with learning. Figure 7, *B* and *C*, shows examples of two neurons that exhibit different modulations in activity, relative to baseline, in the PETH before and after learning. The PETH are plotted with $time\ 0$ denoting the start of the odor investigation epoch. To determine whether the modulations in activity during the trial start and odor investigation epochs were significantly different, we computed the epoch-related activity *relative to baseline* sepa-

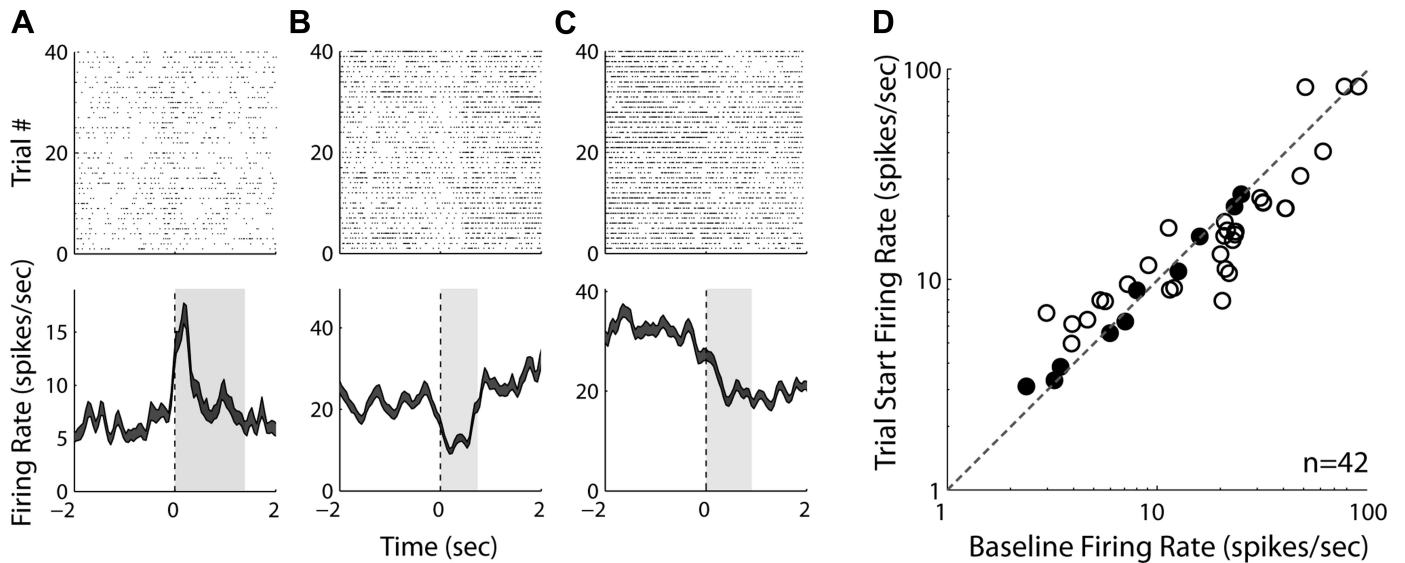


Fig. 5. Neural activity in the HDB/MCPO related to the start of a trial. *A–C*: rasters (*top panels*) and PETH (*bottom panels*) aligned to the start of the trial for 3 neurons in the HDB/MCPO. Neurons in *A* and *B* exhibited phasic increases and decreases during the trial start epoch, respectively, whereas the neuron in *C* shows a nonmonotonic decrease that was locked to the start of the trial but persisted throughout the remainder of the trial. The gray-shaded region in the *bottom panels* represents the average duration of the odor investigation epoch, computed across all trials in the session. *D*: firing rate in the trial start epoch vs. baseline for all neurons in the population. Open circles indicate points that are significantly different from baseline ($P < 0.05$, paired t -test); filled circles are units that did not show significant change in firing rate during odor epoch.

rately for pre- and post-criterion groups of trials, and then tested for significant differences in the relative firing rate changes. Results showed that a fraction of neurons exhibited statistically significant reductions in activity relative to baseline in the odor investigation epoch (6/42, t -test, $P < 0.05$), although no neurons exhibited significant reductions during the approach epoch. As well, we found one neuron that exhibited statistically significant increases in activity post-learning in both the trial start and odor investigation epochs. To summarize the changes in epoch-related activity

across the population, we plotted postcriterion vs. precriterion changes in firing rate separately for the trial start and odor investigation epochs (Fig. 7*D*). The filled symbols correspond to units that exhibited significant changes with learning. Together, these results suggest that neurons in the HDB/MCPO not only exhibit a general decrease in overall firing rate but also can exhibit less substantial fluctuations around baseline once an animal has learned an odor discrimination problem, and are consistent with the notion that projections from the HDB/MCPO to the olfactory system

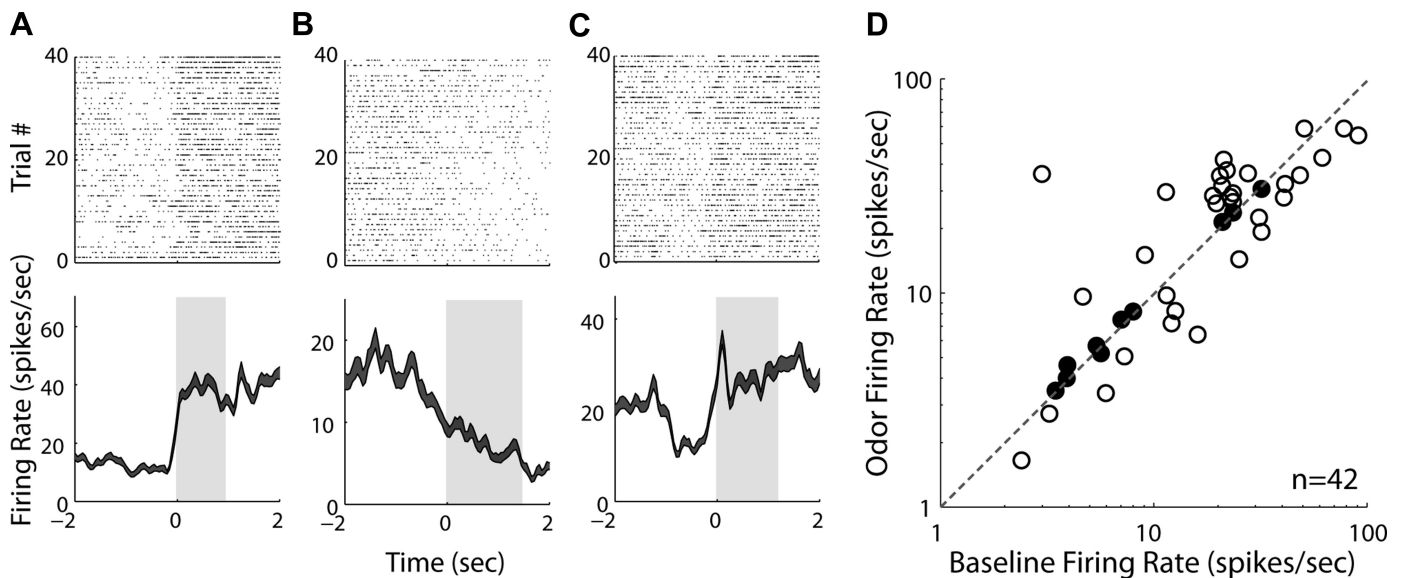


Fig. 6. Neural activity in the HDB/MCPO related to odor investigation. *A–C*: rasters (*top panels*) and PETH (*bottom panels*) aligned to the start of odor investigation for 3 neurons in the HDB/MCPO. Neurons in *A* and *B* exhibited monotonic increases and decreases during the odor investigation epoch, respectively, whereas the neuron in *C* shows a phasic increase locked to the start of the epoch. The gray-shaded region in the *bottom panels* represents the average duration of the odor investigation epoch, computed across all trials in the session. *D*: firing rate in the odor investigation epoch vs. baseline for all neurons in the population. Open circles indicate points that are significantly different from baseline ($P < 0.05$, paired t -test); filled circles are units that did not show significant change in firing rate during odor epoch.

Table 2. Summary of single-unit response properties during 2AFC odor discrimination task

Change in Firing Rate During Trial Start Epoch	Change in Firing Rate During Odor Epoch			Total
	Increase	Decrease	Not Significant	
Increase	3	1	3	7
Decrease	9	8	3	20
Not Significant	3	8	4	15
Total	15	17	10	42

2AFC, 2-alternative forced choice.

are critical during acquisition of novel olfactory discrimination tasks but are less important for recollection.

DISCUSSION

We present in this article the first data on activity of modulatory neurons in the HDB/MCPO in awake, behaving animals during olfactory processing and learning. We investigated HDB/MCPO neural activity during a spontaneous sensory behavior, investigation of odorants, and during a reward-driven operant task by using odorants as conditioned stimuli. Our recordings suggest that HDB/MCPO neurons exhibit fluctuations in firing rate locked to task-related events including those specific to presentation of olfactory stimuli. In particular, we found that activity in the HDB/MCPO is modulated by odor investigation on a short timescale (seconds) and odor-reward associative learning on a longer timescale (minutes). Slow, task-dependent changes in activity are accompanied by overlying fast reactions to active odor sampling. These results, showing activity modulation during olfactory behaviors, support the idea that HDB/MCPO inputs play a role in modulating olfactory sensory processing and learning (de Almeida et al. 2013; Devore and Linstner 2012; Devore et al. 2014).

Baseline activities in HDB/MCPO neurons were higher during a reward-driven task than during spontaneous investigation, suggesting that these inputs are regulated by task demands (Fig. 4). In the reward-driven task, HDB/MCPO activity decreased significantly after the rats reached criterion performance, i.e., after they have acquired the odor discrimination. Modulatory neurons from the HDB/MCPO project, among other brain regions, to both OB and olfactory cortical areas (Cleland and Linstner 2003; Halasz and Shepherd 1983; Shipley and Ennis 1996). In each of these areas, the role of

these modulatory inputs, with an emphasis on cholinergic and GABAergic modulation, has been studied functionally. Hasselmo and colleagues (Barkai and Hasselmo 1994; Hasselmo and Bower 1992; Hasselmo and Cecik 1996) proposed a specific role for cholinergic modulation in the PC. On one hand, these inputs are crucial for allowing long-term potentiation and learning in this structure (Chapuis and Wilson 2013; Fletcher and Wilson 2002), reflecting the increased overall activity in our HDB/MCPO recordings during odor reward learning compared with spontaneous activity. On the other hand, cholinergic as well as GABAergic modulation allows for presynaptic depression of excitatory synaptic transmission in the PC, which has been proposed to decrease proactive interference between multiple memories (Barkai and Hasselmo 1994; Hasselmo and Bower 1992; Poo and Isaacson 2011; Tang and Hasselmo 1994). GABAergic and cholinergic modulatory inputs from the HDB/MCPO could set the tone between learning and recall modes (de Almeida et al. 2013), reflected in our recordings by the decrease in overall activity observed after rats have learned an odor discrimination and are presumably functioning in “recall” mode.

In the OB, HDB/MCPO modulation has been shown to affect the regulation of mitral cell receptive fields in response to odorants. Specifically, activation of HDB/MCPO cholinergic neurons helps narrow mitral cell receptive fields (Ma and Luo 2012; Rothermel et al. 2014) and as a consequence facilitates the discrimination of similar odorants (Chaudhury et al. 2009; Devore et al. 2014). GABAergic projections from HDB/MCPO have been shown to specifically modulate odor discrimination (Nunez-Parra et al. 2013), whereas genetic deletion of specific GABA receptors on granule cells, presumed to be activated by HDB/MCPO GABAergic projections, also

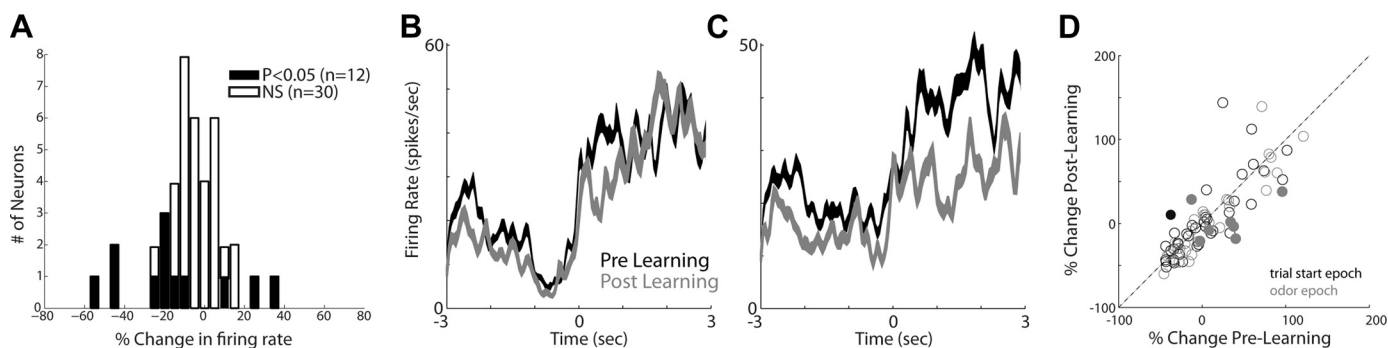


Fig. 7. Neural activity in the HDB/MCPO changes with learning. A: percent change in baseline firing rate for trials completed after animal reaches criterion, expressed as a function of the precriterion baseline firing rate. B and C: learning-related changes in activity in the HDB/MCPO. PETH for 2 neurons (B and C), computed by grouping trials that occurred prelearning (black traces) and postlearning (gray traces), as defined by the trial at which rats achieved criterion performance (defined in MATERIALS AND METHODS). D: epoch-related firing rate (expressed as %change relative to baseline) in postcriterion trials vs. epoch-related firing rate in precriterion trials for each unit recorded in the HDB/MCPO (n = 42). Filled circles are units that show a significant difference between post- and precriterion epoch-related firing rates. Black circles correspond to the trial start epoch and gray circles to the odor investigation epoch.

impairs odor discrimination (Abraham et al. 2010; Nusser et al. 2001). The fast timescale modulation of HDB/MCPO neural activity observed in our recordings could potentially serve to increase the contrast and salience of odors when the rat is investigating the odor. In addition to creating higher contrast representations, modulatory inputs also have been suggested to increase synchrony between responsive mitral cells (Li and Cleland 2013; Nusser et al. 2001), thereby facilitating cortical read out and learning (de Almeida et al. 2013; Devore et al. 2014).

Common modulatory inputs to the OB and cortex have been proposed to serve complementary functions: rapid modulation of representations in the OB accompanied by slower timescale switches between learning and recall in the cortex. As a consequence, modulatory inputs from the HDB/MCPO could serve to both set the tone for learning on the basis of a long timescale as well as modulate odor representations on a shorter timescale. The observations reported presently are consistent with that hypothesis, which is further supported by theoretical and behavioral work.

Basal forebrain projections, and in particular cholinergic projections, have classically been associated with attentional processes (Sarter et al. 2005) and more recently with sensory processing and cue detection (Parikh et al. 2007). Similar to results from olfactory processing, cholinergic inputs are important for visual and auditory receptive field plasticity (Disney et al. 2007; Goard and Dan 2009; Metherate and Weinberger 1989) and stimulus discrimination. Available data suggest that whereas basal forebrain neurons are modulated by macro-level variables such as sleep-wake cycles (Buzsaki et al. 1988; Hassani et al. 2009; Lee et al. 2005), these neurons also show short-term task-dependent modulation during behavioral task in which the animal has to learn stimulus-reward associations (Lin and Nicolelis 2008; Thomson et al. 2014; Tingley et al. 2014, 2015). A recent study by Hangya et al. (2015) showed that in addition to being correlated with attentional processes, neurons in the basal forebrain can be rapidly modulated by aversive as well as appetitive stimuli. In that study, cholinergic neurons in particular were rapidly responsive to aversive and appetitive reinforcement stimuli, suggesting a role for reinforcement learning. Similar to previous studies, the neurons we recorded in the HDB/MCPO did not show uniform modulations during our behavioral tasks, with only some fraction of neurons responding specifically during behavioral epochs and with decreasing or increasing levels of activity (Figs. 2 and 4). Only a fraction of neurons showed the same direction of modulation during different behavioral epochs, leaving open the question as to how increased and decreased firing rates relate to behavior in our data. The diversity of responses could be related to different classes of basal forebrain cells taking on differential roles during learning and recall, as suggest by Hasselmo et al. (1996). Our results are in agreement with recordings from other basal forebrain nuclei (Hangya et al. 2015; Lin and Nicolelis 2008; Thomson et al. 2014; Tingley et al. 2014, 2015) showing a variety of task modulation in basal forebrain neurons. Whereas the tasks chosen in each of these studies are specific to the nucleus under investigation, for example, a selective attention (Tingley et al. 2014, 2015) or tactile discrimination (Thomson et al. 2014), certain task events such as trial start, reward expectations, and motor activity are common to most behavioral tasks. It is therefore

not surprising that common elements can be observed in different basal forebrain nuclei, which may reflect general task processes rather than modality specific responses. Given that the nucleus we record from is the main source of basal forebrain inputs to olfactory structures (Zaborsky et al. 1986), it is to be expected that these neurons are modulated by the investigation and detection of olfactory stimuli and reflect at least to some degree olfactory-specific dynamics. In summary, we show that modulatory inputs from the HDB/MCPO to olfactory structures, both cholinergic and GABAergic, exhibit both fast transient activity changes in response to odor investigation and slower overall modulation in response to task demands.

ACKNOWLEDGMENTS

We thank Matthew Einhorn for technical support.

GRANTS

This research was supported by National Institute of Deafness and Other Communications Disorders Grants R01 DC009948 (to C. Linster), R21 DC009948 (to C. Linster and D. M), and F32 DC011974 (to S. Devore) and a L'Oreal USA Fellowship for Women in Science (to S. Devore).

DISCLOSURES

No conflicts of interest, financial or otherwise, are declared by the authors.

AUTHOR CONTRIBUTIONS

S.D., N.P.-M., D.S., and C.L. conception and design of research; S.D., N.P.-M., and O.D. performed experiments; S.D., N.P.-M., and O.D. analyzed data; S.D., N.P.-M., O.D., D.S., and C.L. interpreted results of experiments; S.D. prepared figures; S.D. drafted manuscript; S.D., N.P.-M., D.S., and C.L. edited and revised manuscript; S.D., N.P.-M., O.D., D.S., and C.L. approved final version of manuscript.

REFERENCES

- Abraham NM, Egger V, Shimshek DR, Renden R, Fukunaga I, Sprengel R, Seeburg PH, Klugmann M, Margrie TW, Schaefer AT, Kuner T. Synaptic inhibition in the olfactory bulb accelerates odor discrimination in mice. *Neuron* 65: 399–411, 2010.
- Barkai E, Hasselmo ME. Modulation of the input/output function of rat piriform cortex pyramidal cells. *J Neurophysiol* 72: 644–658, 1994.
- Brashear HR, Zaborsky L, Heimer L. Distribution of GABAergic and cholinergic neurons in the rat diagonal band. *Neuroscience* 17: 439–451, 1986.
- Buzsaki G, Bickford RG, Ponomareff G, Thal LJ, Mandel R, Gage FH. Nucleus basalis and thalamic control of neocortical activity in the freely moving rat. *J Neurosci* 8: 4007–4026, 1988.
- Chapuis J, Wilson DA. Cholinergic modulation of olfactory pattern separation. *Neurosci Lett* 545: 50–53, 2013.
- Chaudhury D, Escanilla O, Linster C. Bulbar acetylcholine enhances neural and perceptual odor discrimination. *J Neurosci* 29: 52–60, 2009.
- Churchland P, Sejnowski T. Perspectives on cognitive neuroscience. *Science* 242: 741–745, 1988.
- Cleland TA, Linster C. Central olfactory processing. In: *Handbook of Olfaction and Gustation*, edited by Doty RL. New York: Marcel Dekker, 2003, p. 165–180.
- Cleland TA, Morse A, Yue EL, Linster C. Behavioral models of odor similarity. *Behav Neurosci* 116: 222–231, 2002.
- de Almeida L, Idiart M, Linster C. A model of cholinergic modulation in olfactory bulb and piriform cortex. *J Neurophysiol* 109: 1360–1377, 2013.
- De Rosa E, Hasselmo ME, Baxter MG. Contribution of the cholinergic basal forebrain to proactive interference from stored odor memories during associative learning in rats. *Behav Neurosci* 115: 314–327, 2001.

- Devore S, de Almeida L, Linster C.** Distinct roles of bulbar muscarinic and nicotinic receptors in olfactory discrimination learning. *J Neurosci* 34: 11244–11260, 2014.
- Devore S, Linster C.** Noradrenergic and cholinergic modulation of olfactory bulb sensory processing. *Front Behav Neurosci* 6: 52, 2012.
- Devore S, Manella LC, Linster C.** Blocking muscarinic receptors in the olfactory bulb impairs performance on an olfactory short-term memory task. *Front Behav Neurosci* 6: 59, 2012.
- Disney AA, Aoki C, Hawken MJ.** Gain modulation by nicotine in macaque V1. *Neuron* 56: 701–713, 2007.
- Fletcher ML, Chen WR.** Neural correlates of olfactory learning: critical role of centrifugal neuromodulation. *Learn Mem* 17: 561–570, 2010.
- Fletcher ML, Wilson DA.** Experience modifies olfactory acuity: acetylcholine-dependent learning decreases behavioral generalization between similar odorants. *J Neurosci* 22: RC201, 2002.
- Gilbert CD, Sigman M.** Brain states: top-down influences in sensory processing. *Neuron* 54: 677–696, 2007.
- Goard M, Dan Y.** Basal forebrain activation enhances cortical coding of natural scenes. *Nat Neurosci* 12: 1444–1449, 2009.
- Gritti I, Mainville L, Mancina M, Jones BE.** GABAergic and other noncholinergic basal forebrain neurons, together with cholinergic neurons, project to the mesocortex and isocortex in the rat. *Neuroscience* 85: 149–178, 1998.
- Gritti I, Manns ID, Mainville L, Jones BE.** Parvalbumin, calbindin, or calretinin in cortically projecting and GABAergic, cholinergic, or glutamatergic basal forebrain neurons of the rat. *J Comp Neurol* 458: 11–31, 2003.
- Halasz N, Shepherd GM.** Neurochemistry of the vertebrate olfactory bulb. *Neuroscience* 10: 579–619, 1983.
- Hangya B, Ranade SP, Lorenc M, Kepecs A.** Central cholinergic neurons are rapidly recruited by reinforcement feedback. *Cell* 162: 1155–1168, 2015.
- Hassani OK, Lee MG, Henny P, Jones BE.** Discharge profiles of identified GABAergic in comparison to cholinergic and putative glutamatergic basal forebrain neurons across the sleep-wake cycle. *J Neurosci* 29: 11828–11840, 2009.
- Hasselmo ME, Bower JM.** Cholinergic suppression specific to intrinsic not afferent fiber synapses in rat piriform (olfactory) cortex. *J Neurophysiol* 67: 1222–1229, 1992.
- Hasselmo ME, Cekic M.** Suppression of synaptic transmission may allow combination of associative feedback and self-organizing feedforward connections in the neocortex. *Behav Brain Res* 79: 153–161, 1996.
- Hasselmo ME, Schnell E, Barkai E.** Dynamics of learning and recall at excitatory recurrent synapses and cholinergic modulation in rat hippocampal region CA3. *J Neurosci* 15: 5249–5262, 1996.
- Lamour Y, Dutar P, Jobert, A.** Cortical projections of the nucleus of the diagonal band of Broca and of the substantia innominata in the rat: an anatomical study using the anterograde transport of a conjugate of wheat germ agglutinin and horseradish peroxidase. *Neuroscience* 12: 395–408, 1984.
- Lee MG, Hassani OK, Alonso A, Jones BE.** Cholinergic basal forebrain neurons burst with theta during waking and paradoxical sleep. *J Neurosci* 25: 4365–4369, 2005.
- Li G, Cleland TA.** A two-layer biophysical model of cholinergic neuromodulation in olfactory bulb. *J Neurosci* 33: 3037–3058, 2013.
- Lin SC, Nicolelis MA.** Neural ensemble bursting in the basal forebrain encodes salience irrespective of valence. *Neuron* 59: 138–149, 2008.
- Linster C, Cleland TA.** Cholinergic modulation of sensory representations in the olfactory bulb. *Neural Neww* 15: 709–717, 2002.
- Linster C, Garcia PA, Hasselmo ME, Baxter MG.** Selective loss of cholinergic neurons projecting to the olfactory system increases perceptual generalization between similar, but not dissimilar, odorants. *Behav Neurosci* 115: 826–833, 2001.
- Linster C, Hasselmo ME.** Neural activity in the horizontal limb of the diagonal band of Broca can be modulated by electrical stimulation of the olfactory bulb and cortex in rats. *Neurosci Lett* 282: 157–160, 2000.
- Luiten PG, Gaykema RP, Traber J, Spencer DG Jr.** Cortical projection patterns of magnocellular basal nucleus subdivisions as revealed by anterogradely transported *Phaseolus vulgaris* leucoagglutinin. *Brain Res* 413: 229–250, 1987.
- Ma M, Luo M.** Optogenetic activation of basal forebrain cholinergic neurons modulates neuronal excitability and sensory responses in the main olfactory bulb. *J Neurosci* 32: 10105–10116, 2012.
- Mandairon N, Ferretti CJ, Stack CM, Rubin DB, Cleland TA, Linster C.** Cholinergic modulation in the olfactory bulb influences spontaneous olfactory discrimination in adult rats. *Eur J Neurosci* 24: 3234–3244, 2006.
- Metherate R, Weinberger NM.** Acetylcholine produces stimulus-specific receptive field alterations in cat auditory cortex. *Brain Res* 480: 372–377, 1989.
- Nunez-Parra A, Maurer RK, Krahe K, Smith RS, Araneda RC.** Disruption of centrifugal inhibition to olfactory bulb granule cells impairs olfactory discrimination. *Proc Natl Acad Sci USA* 110: 14777–14782, 2013.
- Nusser Z, Kay LM, Laurent G, Homanics GE, Mody I.** Disruption of GABA_A receptors on GABAergic interneurons leads to increased oscillatory power in the olfactory bulb network. *J Neurophysiol* 86: 2823–2833, 2001.
- Parikh V, Kozak R, Martinez V, Sarter M.** Prefrontal acetylcholine release controls cue detection on multiple timescales. *Neuron* 56: 141–154, 2007.
- Pavesi E, Gooch A, Lee E, Fletcher ML.** Cholinergic modulation during acquisition of olfactory fear conditioning alters learning and stimulus generalization in mice. *Learn Mem* 20: 6–10, 2013.
- Paxinos G, Watson C.** *The Rat Brain in Stereotaxic Coordinates*. Amsterdam: Elsevier, 2007.
- Poo C, Isaacson JS.** A major role for intracortical circuits in the strength and tuning of odor-evoked excitation in olfactory cortex. *Neuron* 72: 41–48, 2011.
- Rothermel M, Carey RM, Puche A, Shipley MT, Wachowiak M.** Cholinergic inputs from basal forebrain add an excitatory bias to odor coding in the olfactory bulb. *J Neurosci* 34: 4654–4664, 2014.
- Sarter M, Hasselmo ME, Bruno JP, Givens B.** Unraveling the attentional functions of cortical cholinergic inputs: interactions between signal-driven and cognitive modulation of signal detection. *Brain Res Brain Res Rev* 48: 98–111, 2005.
- Shipley MT, Ennis M.** Functional organization of olfactory system. *J Neurobiol* 30: 123–176, 1996.
- Tang AC, Hasselmo ME.** Selective suppression of intrinsic but not afferent fiber synaptic transmission by baclofen in the piriform (olfactory) cortex. *Brain Res* 659: 75–81, 1994.
- Thomson E, Lou J, Sylvester K, McDonough A, Tica S, Nicolelis MA.** Basal forebrain dynamics during a tactile discrimination task. *J Neurophysiol* 112: 1179–1191, 2014.
- Tingley D, Alexander AS, Kolbu S, de Sa VR, Chiba AA, Nitz DA.** Task-phase-specific dynamics of basal forebrain neuronal ensembles. *Front Syst Neurosci* 8: 174, 2014.
- Tingley D, Alexander AS, Quinn LK, Chiba AA, Nitz DA.** Cell assemblies of the basal forebrain. *J Neurosci* 35: 2992–3000, 2015.
- Wilson DA, Fletcher ML, Sullivan RM.** Acetylcholine and olfactory perceptual learning. *Learn Mem* 11: 28–34, 2004.
- Wilson DA, Linster C.** Neurobiology of a simple memory. *J Neurophysiol* 100: 2–7, 2008.
- Záborszky L, Carlsen J, Brashear HR, Heimer L.** Cholinergic and GABAergic afferents to the olfactory bulb in the rat with special emphasis on the projection neurons in the nucleus of the horizontal limb of the diagonal band. *J Comp Neurol* 243: 488–509, 1986.
- Zaborszky L, Csordas A, Mosca K, Kim J, Gielow MR, Vadasz C, Nadasdy Z.** Neurons in the basal forebrain project to the cortex in a complex topographic organization that reflects corticocortical connectivity patterns: an experimental study based on retrograde tracing and 3D reconstruction. *Cereb Cortex* 25: 118–137, 2015.
- Zaborszky L, Pang K, Somogyi J, Nadasdy Z, Kallo I.** The basal forebrain corticopetal system revisited. *Ann NY Acad Sci* 877: 339–367, 1999.